JOURNAL OF GYNECOLOGIC ONCOLOGY

Original Article

Check for updates

LncRNA XIST promotes carboplatin resistance of ovarian cancer through activating autophagy via targeting miR-506-3p/FOXP1 axis

Xiaoyan Xia (iD),[1] Zikui Li (iD),[2] Yaojun Li (iD),[3] Feng Ye (iD),[3] Xiaoming Zhou (iD) [4]

[1]Scientific Research Department, Changsha Health Vocational College, Changsha, P.R. China
[2]Department of Obstetrics and Gynecology, The Fist Hospital of Hunan University of Chinese Medicine, Changsha, P.R. China
[3]Nursing College of Changsha Health Vocational College, Changsha, P.R. China
[4]Department of Cardiology, The Fist Hospital of Hunan University of Chinese Medicine, Changsha, P.R. China

OPEN ACCESS

Correspondence to
Xiaoming Zhou
Department of Cardiology, The Fist Hospital of Hunan University of Chinese Medicine, No. 95, Shaoshan Middle Road, Changsha 410007, P.R. China.
Email: 43960905@qq.com

ORCID iDs
Xiaoyan Xia (iD)
https://orcid.org/0000-0002-7661-5445
Zikui Li (iD)
https://orcid.org/0000-0002-0334-834X
Yaojun Li (iD)
https://orcid.org/0000-0002-6196-6218

ABSTRACT

Objective: Resistance to chemotherapy drugs makes ovarian cancer (OC) difficult to treat and ultimately kills patients. Long non-coding RNAs are closely related to carboplatin resistance in OC. In present study, we explored the role of lncRNA X-inactive specific transcript (XIST) on carboplatin resistance in OC.

Methods: Cell viability, proliferation, and apoptosis were assessed through 2,5-diphenyl-2H-tetrazolium bromide, colony formation, and flow cytometry assays, respectively. Microtubule-associated protein 1A/1B-light chain 3 expression was evaluated by immunofluorescence assay to analyze the cell autophagy. The interaction of XIST/miR-506-3p or miR-506-3p/forkhead box protein P1 (FOXP1) was analyzed using RNA immunoprecipitation (RIP) and dual-luciferases reporter assays. The function of XIST/miR-506-3p/FOXP1 axis in vivo was further confirmed by tumor xenograft study and immunohistochemistry.

Results: The expression of XIST and FOXP1 increased while miR-506-3p decreased in OC and carboplatin resistance cells. XIST silencing repressed the proliferative and autophagic capacities of carboplatin resistance cells while promoted the apoptosis. XIST overexpression led to the opposite results. XIST targeted miR-506-3p and downregulated its expression. MiR-506-3p inhibition facilitated the proliferative and autophagic capacities while suppressed the apoptosis of cells, XIST knockdown reversed these effects. MiR-506-3p bound to FOXP1. XIST knockdown or miR-506-3p overexpression reversed the increase of cell proliferative and autophagic abilities and the decrease of apoptosis rate induced by FOXP1 overexpression. XIST affected autophagy and carboplatin resistance in vivo via regulating the miR-506-3p/FOXP1 axis.

Conclusion: XIST knockdown inhibited autophagy and carboplatin resistance of OC through FOXP1/protein kinase B (AKT)/mammalian target of rapamycin pathway by targeting miR-506-3p.

Keywords: Ovarian Cancer; Carboplatin

Generated by xmlinkpress

Feng Ye (iD)
https://orcid.org/0000-0002-1947-9467
Xiaoming Zhou (iD)
https://orcid.org/0000-0003-1189-6677

Conflict of Interest
No potential conflict of interest relevant to this article was reported.

Author Contributions
Conceptualization: X.X., Z.X.; Data curation: X.X., L.Z., Y.F.; Formal analysis: L.Y., Y.F.; Funding acquisition: Z.X.; Investigation: X.X.; Methodology: X.X.; Project administration: Z.X.; Resources: L.Z.; Software: L.Y.; Supervision: Z.X.; Validation: X.X.; Visualization: X.X.; Writing - original draft: X.X., Z.X. Writing - review & editing: X.X., Z.X.

Synopsis

Knockdown of XIST inhibited autophagy induced by carboplatin and resistance to carboplatin in ovarian cells. XIST targeted miR-506-3p and reduced its expression. FOXP1 could be a target gene of miR-506-3p. XIST facilitated the autophagy and carboplatin resistance through miR-506-3p/FOXP1 axis in ovarian cancer.

INTRODUCTION

Ovarian cancer (OC) is the main cause of gynecological cancer mortality in most developed countries. It does not only let women and family into physical and psychologic agony, but also cause serious social and economic load [1,2]. Currently, the most frequent treatment for OC is a combination of surgery and chemotherapy drugs. Although the development and popularization of chemotherapy drugs such as cisplatin and carboplatin have extended the survival time of OC patients to some extent [3], the long-term use of chemical drugs can cause cancer cells to develop drug resistance, so that many patients die from recurrent and progressive diseases [4]. Therefore, it is very important to explore and discover molecular targets for regulating chemotherapy resistance in OC.

Long non-coding RNAs (lncRNAs), which play a role in the control of several tumor cell activities, such as proliferation, apoptosis, autophagy, epithelial-mesenchymal transition (EMT) and drug resistance, are possible markers for a range of human cancers [5]. In recent years, a growing body of evidence showed that lncRNA X-inactive specific transcript (XIST) was abnormally expressed in tumors and controlled the progression of multiple cancers [6], such as thyroid cancer [7]. Furthermore, the function of XIST in chemoresistance have gotten a lot of attention and have been widely explored. A previous study explored the mechanism by which carboplatin combined with XIST worked against retinoblastoma, and demonstrated that carboplatin could suppress cell proliferation and EMT in vitro by regulating the XIST/miR-200a-3p/Neuropilin 1 pathway [8]. It was reported that XIST was highly expressed in OC both in vivo and in vitro, which was linked to tumor grade and distant metastasis [9]. However, there are few studies on whether the combination of carboplatin and XIST can regulate the development of OC cells, which may be a potential therapeutic method. Thus, this study was to establish a theoretical foundation for the implementation of carboplatin and XIST targeted therapy from the perspective of molecular biology.

MicroRNAs (miRNAs) were proved to regulate fundamental cellular processes and tissue specific functions through post-transcriptionally regulating gene expression by binding to 3'-untranslated region (3'-UTR) of mRNAs [10,11]. Overexpression of miR-506-3p has been observed to suppress certain human tumors, including OC. For instance, miR-506-3p enhancement was suggested to act as a way to prevent the onset of OC [12]. Moreover, miR-506-3p was found to regulate autophagic and proliferative processes in post-burn skin fibroblasts by inhibiting Beclin-1 level [13]. MiR-506-3p enhanced cisplatin sensitivity in serous OC by regulating the Enhancer of zeste homolog 2/β-catenin pathway [14]. On the other hand, the role of miR-506-3p in OC carboplatin resistance needs to be further studied. Forkhead box protein P1 (FOXP1), a member of the FOXP subfamily of transcription factors, was found to be up-regulated in OC, and miR-29c-3p suppressed autophagy and drug resistance in OC cells by down-regulating FOXP1 [15]. Furthermore, protein kinase B (AKT)/mammalian target of the rapamycin (mTOR) pathway was extremely actived in OC,

regulating a range of cellular functions and playing a key role in OC development [16]. It has also been reported that FOXP1 can stimulate AKT/mTOR pathway [17]. Therefore, the regulatory mechanism of the FOXP1/AKT/mTOR axis in OC is worth exploring.

The function of the crosstalk of XIST, miR-506-3p and FOXP1 on OC cell growth, autophagy and carboplatin resistance was explored in this work. Our findings provided a feasible theoretical basis for increasing carboplatin sensitivity in OC therapy.

MATERIALS AND METHODS

1. Cell lines and treatment

Human ovarian surface epithelial cells HOSE and OC cells SKOV3, A2780 and HO-8910 were offered by American Type Culture Collection (ATCC, Manassas, VA, USA), then maintained in Roswell Park Memorial Institute-1640 (Invitrogen, Carlsbad, CA, USA) supplemented with 10% fetal bovine serum (FBS, Invitrogen), 100 U/mL penicillin and 100 μg/mL streptomycin (Invitrogen) at 37℃ with 5% CO_2.

SKOV3 and A2780 cells were transfected with the following plasmids: short hairpin RNA XIST (sh-XIST), XIST overexpression (OE-XIST), miR-506-3p mimics, miR-506-3p inhibitor, and OE-FOXP1 alone or in combination: miR-506-3p inhibitor+sh-XIST, OE-FOXP1+miR-506-3p mimics, OE-FOXP1+sh-XIST and the corresponding negative controls using Lipofectamine 3000 (Invitrogen). All plasmids were purchased from RiboBio (Guangzhou, China).

2. Quantitative real-time-polymerase chain reaction (qRT-PCR)

Total RNA was isolated by TRIzol reagent (Invitrogen), then RNA quality was detected using NanoDro2000c (Thermo Scientific, Waltham, MA, USA). Next, TaqMan® miRNA reverse transcription kit was employed in miRNA qPCR assay, and for the other genes, random primers from the RT Master Mix kit were used to synthesize cDNAs, and qRT-PCR process was performed on an ABI 7900 system using SYBR Green Real-Time PCR master mixes (Thermo). The relative expressions were normalized to that of glyceraldehyde 3-phosphate dehydrogenase (GAPDH) mRNA or U6 using the $2^{-\Delta\Delta Ct}$ method. Primers were showed in **Table S1**.

3. Western blot

Total proteins were isolated, and the concentration was determined using BCA method. After proteins was separated by using 10%–12% SDS-PAGE, proteins were transferred to PVDF membranes (Millipore, Bedford, MA, USA). The 1% BSA in TBS buffer was used to block the membranes and cultivated at 4℃ overnight with primary antibodies against FOXP1 (1:5,000, ab134055, Abcam, Cambridge, UK), microtubule-associated protein 1A/1B-light chain 3 (LC3) (1:3,000, ab51520), P62 (1:1,000, ab207305), B-cell lymphoma 2 (Bcl-2) (1:1,000, ab59348), Bcl-2 associated X (Bax) (1:5,000, ab32503), AKT (1:500, ab8805), phospho (p)-AKT (1:1,000, ab38449), mTOR (1:10,000, ab134903), GAPDH (1:1,000, ab8245), β-actin (1:1,000, ab8226). Then incubating with the corresponding secondary antibodies. The protein signaling was visualized by ECL reagent. GAPDH and β-actin as loading controls and all antibodies were purchased from Abcam.

4. 2,5-diphenyl-2H-tetrazolium bromide (MTT) assay

Cells (5,000/well) were seeded into 96-well plates and incubated for 24 hours, then treated with carboplatin at different concentrations (0, 100, 150, 200, 250, 300 μM). After incubating

for 48 hours, cells were cultured with MTT solution at 37°C and then dissolved in dimethyl sulfoxide. Cell viability was detected at 570 nm by a microplate reader (BioTek Instruments, Winooski, VT, USA).

5. Colony formation assay

Cells seeded into 6-well plates were cultured at 37°C until 100% confluence. The medium was changed every 2 days. After 14 days, the colonies were fixed with 4% paraformaldehyde and then stained with 0.1% crystal violet. A microscope was used to calculate the number of colonies.

6. Flow cytometry

Cells were washed with binding buffer and then centrifuged at 500 × g for 5 minutes at room temperature, then resuspended in cold PBS. Next, 10 μL Annexin V-fluorescein isothiocyanate and 10 μL propidium iodide were added and cultured for 15 min in the dark. Samples were analyzed through Becton-Dickinson flow cytometer.

7. Immunofluorescence assay

After fixing with 4% formaldehyde, cells were cultured with 5% Tris buffered saline with Tween-20 (pH 8.3) diluted non-fat dry milk and incubated with the primary antibody LC3 (1:2,000, ab51520, Abcam) and corresponding secondary antibody. Next, 4',6-diamidino-2-phenylindole (DAPI) was used to stain cell nuclear, and a confocal laser scanning microscope was used to analyze the immunofluorescence images.

8. RNA immunoprecipitation (RIP) assay

RIP assay was conducted using a Magna RIP™ RNA-Binding Protein Immunoprecipitation Kit (Millipore). Cells were lysed with RIP lysis buffer and then immunoglobulin G (IgG) antibody and argonaute 2 (Ago2) antibody coated on magnetic beads overnight. Then the RNA complexes were purified. The co-precipitated RNA was extracted using TRIzol™, and qRT-PCR was then used to analyze the purified RNA.

9. Dual-luciferase reporter assay

Briefly, the wild type (WT) putative miR-506-3p binding site of the XIST or FOXP1 3'-UTR was amplified and inserted into the pmirGLO vectors to establish recombinant luciferase reporter plasmids and named XIST-WT or FOXP1-WT. The matched mutant (MUT) miR-506-3p binding site was also cloned into the pmirGLO vectors to establish mutant recombinant luciferase reporter plasmids and named XIST-MUT or FOXP1-MUT. Then, cells were co-transfected with above plasmids and miR-506-3p mimics or mimics NC for 24 hours. Finally, luciferase intensity was tested by Dual-Luciferase Reporter Assay System (Promega, Madison, WI, USA).

10. Tumor xenograft model

BALB/c-nude mice (22–24 g, 6 weeks) were purchased from Animal Experiment Center of Chinese Academy of Sciences (Shanghai, China). SKOV3 cells stably expressed sh-NC, sh-XIST, sh-NC+CBP and sh-XIST+CBP were injected subcutaneously into the right flank of the mice (n=6) to perform tumorigenesis assay. Then we measured the tumor size using calipers every 5 days and calculated the volume. After 20 days, mice were sacrificed, and then xenograft tumor tissues were harvested. All experiments were performed according to protocols from the Frist Hospital of Hunan University of Chinese Medicine and approved by the Frist Hospital of Hunan University of Chinese Medicine and the Laboratory Animal Ethics Committee, which conforms to the relevant provisions of the National Laboratory Animal Welfare ethics.

11. Immunohistochemistry

Paraffin sections were deparaffinized and hydrated. After serial incubation with primary antibodies anti-LC3 (1:400, ab48394, Abcam), anti-cleaved caspase3 (1:50, #9661, Cell signaling, Danvers, MA, USA) and secondary antibody, then subjected to the liquid DAB substrate-chromogen system. Images were visualized using a Nikon ECLIPSE Ti microscope system and processed with Nikon software.

12. Statistical analysis

All data was presented as mean ± standard deviation. Data analysis was performed by Graphpad Prism (Version 7.0; San Diego, CA, USA) using Student's t test or one-way analysis of variance. The value of p less than 0.05 was considered significant.

RESULTS

1. XIST and FOXP1 were highly expressed while miR-506-3p decreased in OC cells

QRT-PCR was used to reconfirm the abnormal expression of XIST in OC cells. As shown in **Fig. 1A**, XIST was increased in SKOV3, A2780 and HO-8910 cells. Conversely, miR-506-3p showed down-regulation in OC cells (**Fig. 1B**). In addition, FOXP1 was observed to be overexpressed in OC cells (**Fig. 1C and D**). SKOV3 and A2780 cells with the most obvious differential expression were selected for subsequent experiments.

2. Knockdown of XIST inhibited the autophagy in vitro, as well as OC cell resistance to carboplatin

To study the biological function of XIST dysregulation in OC carboplatin resistant cells (SKOV3/CBP and A2780/CBP cells), we first measured XIST levels in SKOV3/CBP and A2780/CBP cells and observed that XIST was significantly over expressed (**Fig. 2A**). Subsequently, MTT results showed that as the concentration of carboplatin was increased, cell proliferative
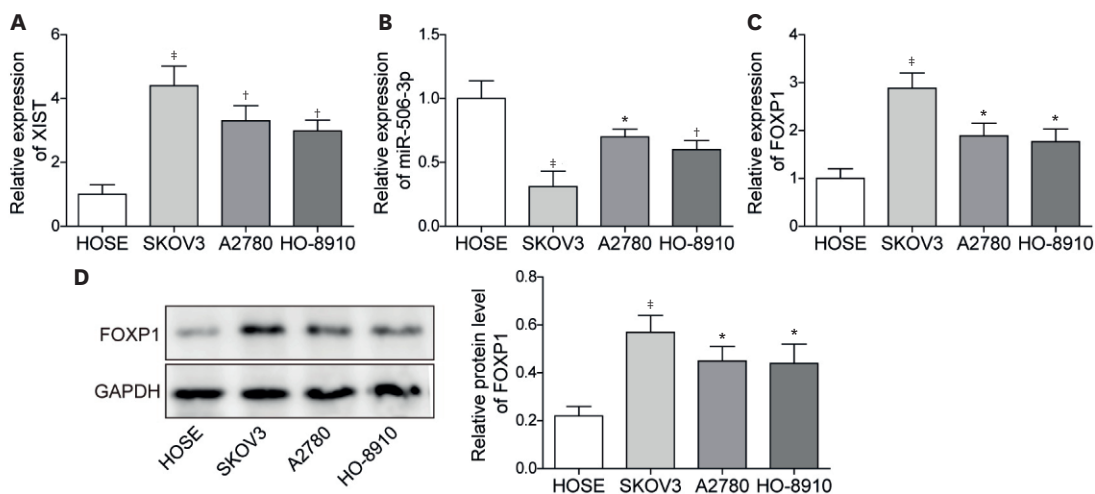

Fig. 1. XIST and FOXP1 were highly expressed while miR-506-3p decreased in OC cells. (A-C) quantitative real-time-polymerase chain reaction evaluated XIST, miR-506-3p and FOXP1 levels in OC cells (SKOV3, A2780 and HO-8910) and normal cells HOSE. (D) The protein level of FOXP1 was assessed by western blot. The experimental data were showed as mean ± SD. n=3.
FOXP1, forkhead box protein P1; GAPDH, glyceraldehyde 3-phosphate dehydrogenase; OC, ovarian cancer; XIST, X-inactive specific transcript.
*p<0.05, †p< 0.01, and ‡p<0.001.

ability dropped progressively (**Fig. 2B**). To determine the impact of XIST knockdown or overexpression on carboplatin sensitivity, we first conducted the transfection efficiencies of sh-XIST and OE-XIST in SKOV3/CBP and A2780/CBP cells and observed that XIST significantly decreased or increased as expected (**Fig. 2C**). Then, the results indicated that knockdown of XIST suppressed the proliferation of carboplatin resistant OC cells, while enhancement of XIST promoted the proliferation (**Fig. 2D**). Furthermore, compared with the apoptosis rate in the control groups, XIST knockdown increased the cell apoptosis, while XIST overexpression reduced the apoptosis (**Fig. 2E**). Silencing of XIST promoted the expression of Bax (pro-apoptosis protein) and inhibited Bcl-2 (anti-apoptotic protein) levels, while overexpression of XIST led to the opposite results (**Fig. 2F**). An immunofluorescence technique was used to analyze the autophagy of SKOV3/CBP and A2780/CBP cells. We observed that knockdown of XIST inhibited cell autophagy, which was further confirmed by the decrease of LC3 II/I level and the increase of P62 level, Conversely, overexpression of XIST promoted cell autophagy (**Fig. 2G-I**). Taken together, XIST facilitated carboplatin resistance in OC cells, while depletion of XIST was able to improve the efficacy of carboplatin.

3. XIST upregulated FOXP1 levels by targeting miR-506-3p

Since the downregulation of miR-506-3p in OC, we had reason to clarify the interaction of XIST/miR-506-3p. StarBase analysis demonstrated a binding sequence between XIST and miR-506-3p (**Fig. 3A**). Then, as shown in **Fig. 3B**, XIST and miR-506-3p were coimmunoprecipitated by Ago2 antibody instead of IgG antibody. Furthermore, co-transfection of XIST-WT and miR-506-3p mimics repressed luciferase activities, while the activities in the XIST-MUT reporter had no significant change (**Fig. 3C**). MiR-506-3p levels were increased after transfecting with sh-XIST or miR-506-3p mimics, while transfection of OE-XIST decreased miR-506-3p levels (**Fig. 3D**). Therefore, we concluded that miR-506-3p was directly bound to XIST. In addition, FOXP1 was found to be over expressed in carboplatin resistant OC cells (**Fig. 3E**). MiR-506-3p enhancement could suppress FOXP1 expression and the protein expression of mTOR and the phosphorylation of AKT (**Fig. 3F and G**). Subsequently, a binding site between miR-506-3p and FOXP1 was found by StarBase (**Fig. 3H**). As shown in **Fig. 3I**, FOXP1-WT co-transfected with miR-506-3p mimics inhibited luciferase activity, while there was no significant change after co-transfecting with FOXP1-MUT and miR-506-3p mimics, which further confirmed the targeted relationship between them. Taken together, XIST might positively regulate FOXP1 expression by targeting miR-506-3p.

4. Knockdown of XIST inhibited the autophagy and OC cell resistance to carboplatin through targeting miR-506-3p

Next, a rescue assay was designed and used in vitro to explore the function of the XIST/miR-506-3p pathway. Firstly, miR-506-3p was down-regulated in carboplatin resistant cells (**Fig. 4A**). Then, we silenced miR-506-3p levels in SKOV3/CBP and A2780/CBP cells (**Fig. 4B**). The proliferation of SKOV3/CBP and A2780/CBP cells was enhanced after knockdown of miR-506-3p, while simultaneous silencing of miR-506-3p and XIST blocked the promoting effects (**Fig. 4C**). In addition, the reduction in apoptosis rate caused by miR-506-3p knockdown was restored through silencing of XIST (**Fig. 4D**). Furthermore, the miR-506-3p inhibitor reduced the level of Bax and enhanced Bcl-2 expression, while knockdown of XIST reversed the effect (**Fig. 4E**). MiR-506-3p silencing increased autophagic cells, while the increase was arrested by co-transfection with sh-XIST (**Fig. 4F**). Knockdown of XIST eliminated the promoting effects of miR-506-3p silencing on LC3 II/I expression and the inhibiting effects on P62 levels (**Fig. 4G and H**). Taken together, the XIST/miR-506-3p pathway did influence carboplatin sensitivity in vitro.
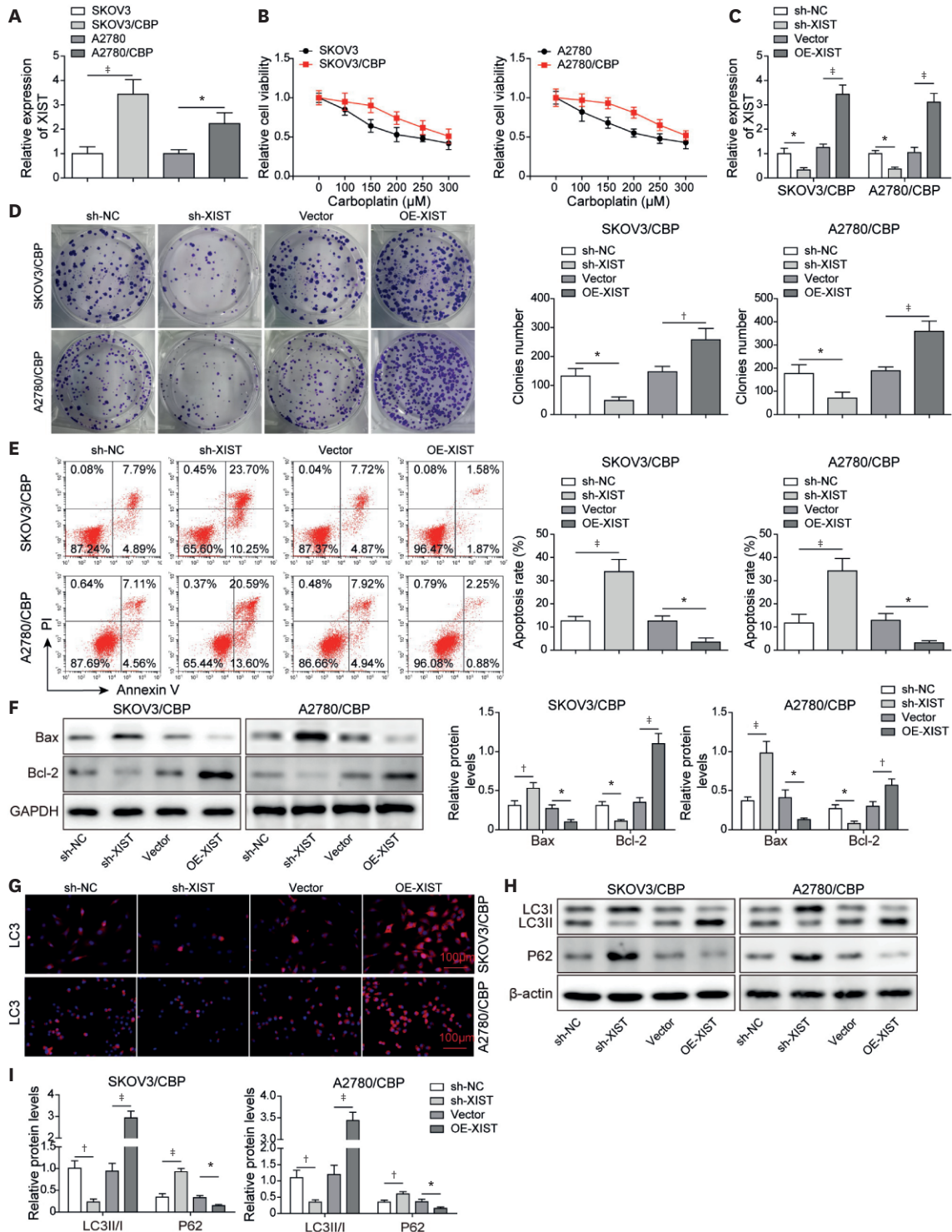
Fig. 2. Knockdown of XIST inhibited the autophagy and the resistance to carboplatin in OC cells. (A) qRT-PCR detected XIST level in carboplatin-resistant cells (SKOV3/CBP, A2780/CBP cells). (B) The cell viability of OC cells was assessed by MTT after treating with different concentration of carboplatin. sh-XIST and OE-XIST transfected into SKOV3/CBP, A2780/CBP cells. (C) qRT-PCR was used to evaluate XIST expression. (D-E) The proliferative ability and apoptotic rate were detected through colony formation, flow cytometry, and respectively. (F) The expression of Bax and Bcl-2 was detected by western blot. (G) The LC3 levels was measured by immunofluorescence assay. (H-I) The proteins expression of LC3 II/I, P62 was detected by western blot. The experimental data were showed as mean ± SD. n=3. Bax, Bcl-2 associated X; Bcl-2, B-cell lymphoma 2; LC3, light chain 3; OC, ovarian cancer; OE-XIST, XIST overexpression; qRT-PCR, quantitative real-time-polymerase chain reaction; sh-NC, short hairpin RNA NC; sh-XIST, short hairpin RNA XIST; XIST, X-inactive specific transcript.
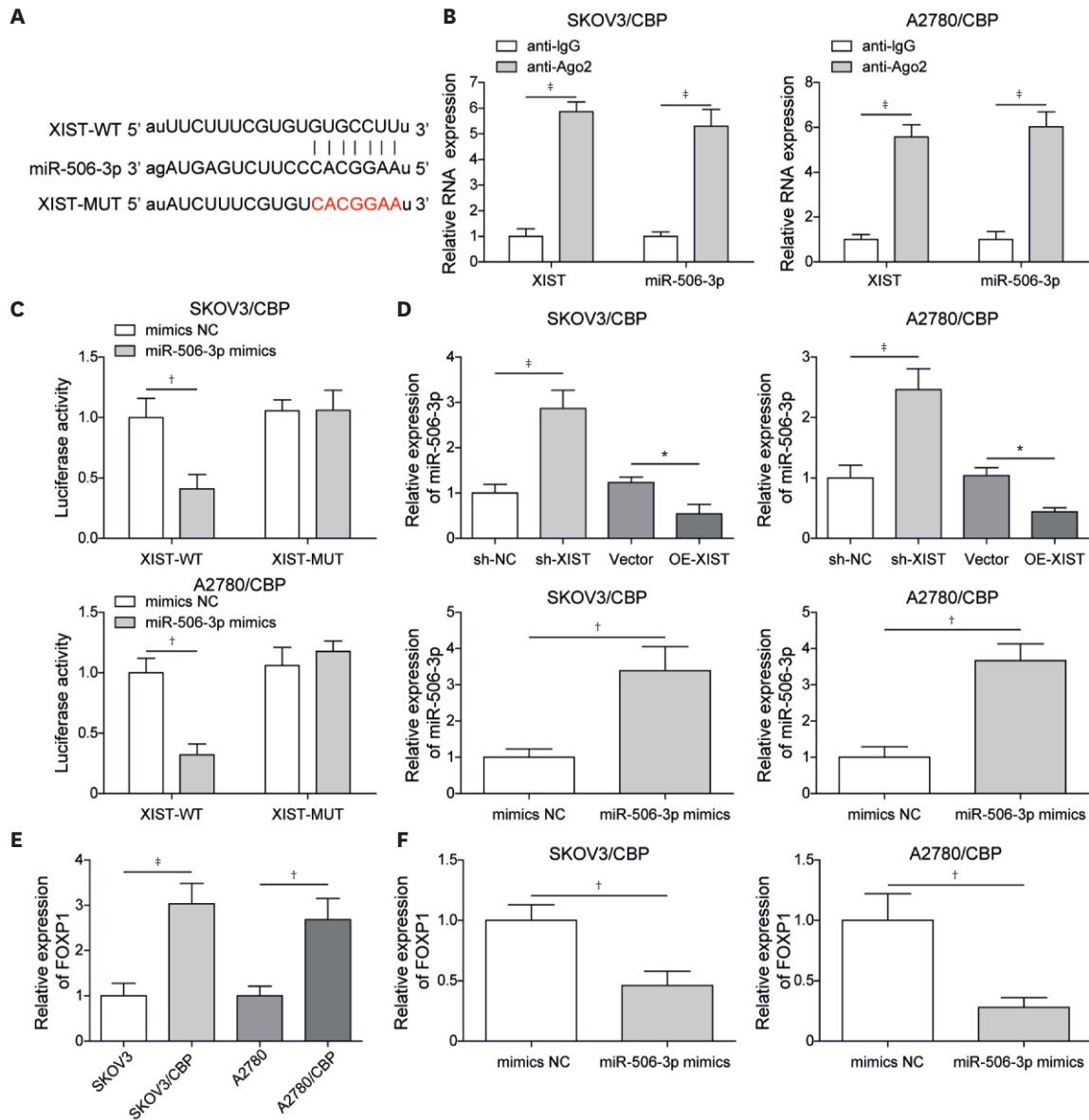*p<0.05, †p< 0.01, and ‡p<0.001.

Fig. 3. XIST up-regulated FOXP1 levels by targeting miR-506-3p. (A) StarBase indicated a binding sequence of XIST/miR-506-3p. (B-C) RNA immunoprecipitation and dual-luciferase reporter assays were used to further validate the regulatory relationship between XIST and miR-506-3p. (D) MiR-506-3p levels were tested using qRT-PCR in SKOV3/CBP and A2780/CBP cells after transfecting with sh-XIST, OE-XIST or miR-506-3p mimics. (E-F) FOXP1 level was assessed via qRT-PCR. (G) FOXP1, AKT, p-AKT and mTOR levels in SKOV3/CBP and A2780/CBP cells transfected with miR-506-3p mimics were evaluated using western blot. (H) The prediction of binding site of FOXP1/miR-506-3p. (I) Dual-luciferase reporter assay further demonstrated the interaction. The data was showed as mean ± SD. n=3. Ago2, argonaute 2; AKT, protein kinase B; FOXP1, forkhead box protein P1; GAPDH, glyceraldehyde 3-phosphate dehydrogenase; IgG, immunoglobulin G; mTOR, mammalian target of rapamycin; MUT, mutant; qRT-PCR, quantitative real-time-polymerase chain reaction; sh-NC, short hairpin RNA NC; sh-XIST, short hairpin RNA XIST; WT, wild type; XIST, X-inactive specific transcript.
*p<0.05, †p< 0.01, and ‡p<0.001.

5. Knockdown of XIST inhibited autophagy while promoting OC cell sensitivity to carboplatin by the regulating the FOXP1/AKT/mTOR pathway via miR-506-3p

To learn more about the impact of the XIST/miR-506-3p/FOXP1 pathway on OC cell sensitivity to carboplatin, we first measured the overexpression efficiency of OE-FOXP1 in SKOV3/CBP and A2780/CBP cells (**Fig. S1A and B**). As shown in **Fig. S1C**, the proliferation of SKOV3/CBP and A2780/CBP cells increased in the OE-FOXP1 group, while the promoting effect of FOXP1
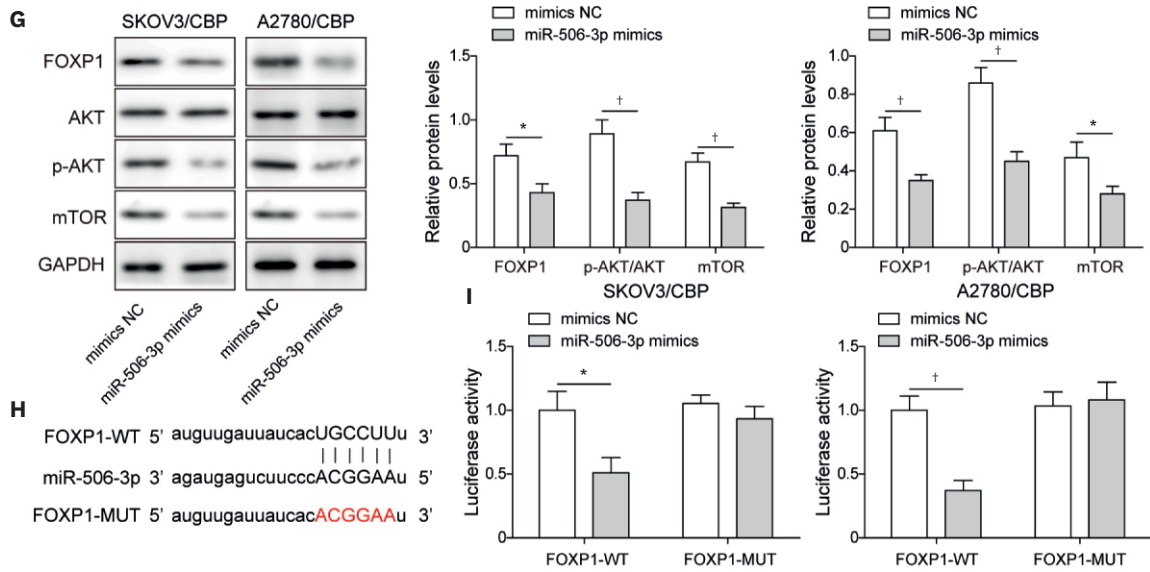
Fig. 3. (Continued) XIST up-regulated FOXP1 levels by targeting miR-506-3p. (A) StarBase indicated a binding sequence of XIST/miR-506-3p. (B-C) RNA immunoprecipitation and dual-luciferase reporter assays were used to further validate the regulatory relationship between XIST and miR-506-3p. (D) MiR-506-3p levels were tested using qRT-PCR in SKOV3/CBP and A2780/CBP cells after transfecting with sh-XIST, OE-XIST or miR-506-3p mimics. (E-F) FOXP1 level was assessed via qRT-PCR. (G) FOXP1, AKT, p-AKT and mTOR levels in SKOV3/CBP and A2780/CBP cells transfected with miR-506-3p mimics were evaluated using western blot. (H) The prediction of binding site of FOXP1/miR-506-3p. (I) Dual-luciferase reporter assay further demonstrated the interaction. The data was showed as mean ± SD. n=3.

Ago2, argonaute 2; AKT, protein kinase B; FOXP1, forkhead box protein P1; GAPDH, glyceraldehyde 3-phosphate dehydrogenase; IgG, immunoglobulin G; mTOR, mammalian target of rapamycin; MUT, mutant; qRT-PCR, quantitative real-time-polymerase chain reaction; sh-NC, short hairpin RNA NC; sh-XIST, short hairpin RNA XIST; WT, wild type; XIST, X-inactive specific transcript.
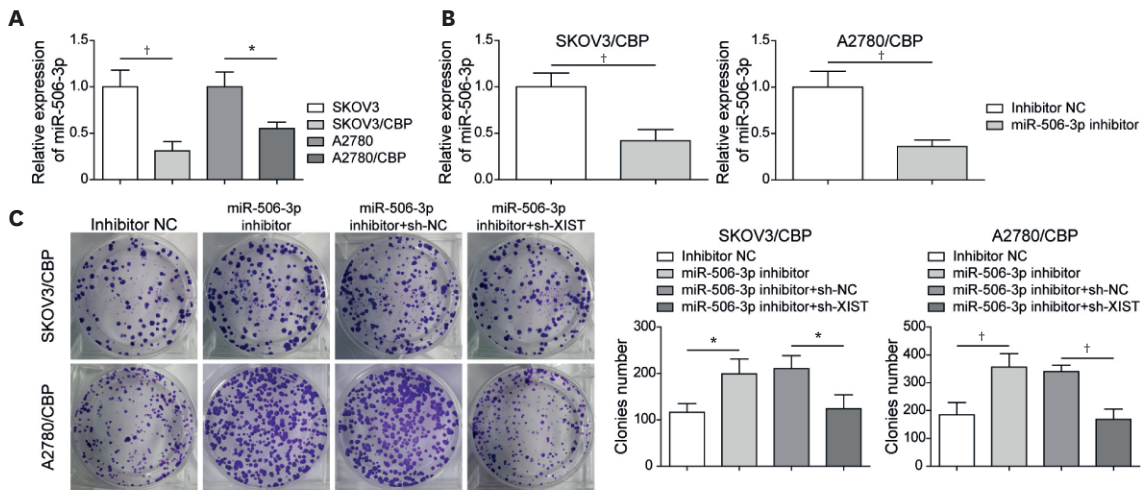
$^{*}p<0.05$, $^{†}p< 0.01$, and $^{‡}p<0.001$.

Fig. 4. Knockdown of XIST inhibited the autophagy in OC cell resistance to carboplatin through targeting miR-506-3p. (A) qRT-PCR evaluated miR-506-3p levels in carboplatin-resistant cells. (B) The expression of miR-506-3p was assessed via qRT-PCR. The SKOV3/CBP and A2780/CBP cells were transfected with miR-506-3p inhibitor or sh-XIST (C-D) The cell viability and apoptosis were tested via colony formation and flow cytometry after silencing miR-506-3p or simultaneously knocking down miR-506-3p and XIST. (E) The levels of Bax and Bcl-2 were detected by western blot. (F) LC3 expression level was measured by immunofluorescence assay. (G-H) LC3 II/I and P62 levels were tested by western blot. The data were showed as mean ± SD. n=3.

Bax, Bcl-2 associated X; Bcl-2, B-cell lymphoma 2; GAPDH, glyceraldehyde 3-phosphate dehydrogenase; LC3, light chain 3; qRT-PCR, quantitative real-time-polymerase chain reaction; sh-NC, short hairpin RNA NC; sh-XIST, short hairpin RNA XIST; XIST, X-inactive specific transcript.

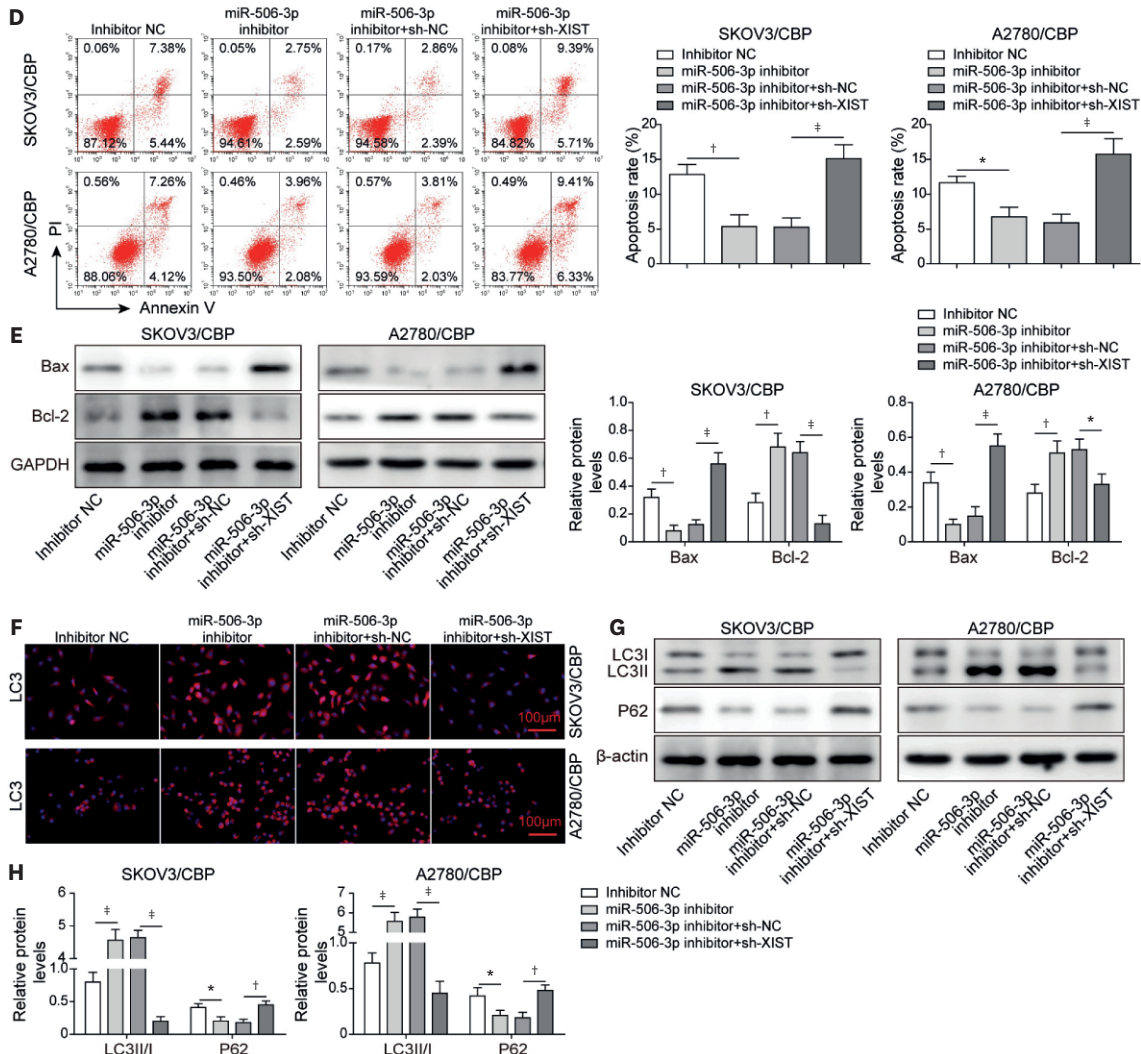$^{*}p<0.05$, $^{†}p< 0.01$, and $^{‡}p<0.001$.

Fig. 4. (Continued) Knockdown of XIST inhibited the autophagy in OC cell resistance to carboplatin through targeting miR-506-3p. (A) qRT-PCR evaluated miR-506-3p levels in carboplatin-resistant cells. (B) The expression of miR-506-3p was assessed via qRT-PCR. The SKOV3/CBP and A2780/CBP cells were transfected with miR-506-3p inhibitor or sh-XIST (C-D) The cell viability and apoptosis were tested via colony formation and flow cytometry after silencing miR-506-3p or simultaneous knocking down miR-506-3p and XIST. (E) The levels of Bax and Bcl-2 were detected by western blot. (F) LC3 expression level was measured by immunofluorescence assay. (G-H) LC3 II/I and P62 levels were tested by western blot. The data were showed as mean ± SD. n=3.
Bax, Bcl-2 associated X; Bcl-2, B-cell lymphoma 2; GAPDH, glyceraldehyde 3-phosphate dehydrogenase; LC3, light chain 3; qRT-PCR, quantitative real-time-polymerase chain reaction; sh-NC, short hairpin RNA NC; sh-XIST, short hairpin RNA XIST; XIST, X-inactive specific transcript.
*p<0.05, †p< 0.01, and ‡p<0.001.

overexpression was reversed through transfecting with miR-506-3p mimics or sh-XIST. Furthermore, miR-506-3p enhancement or XIST silencing abolished the inhibitory effects of FOXP1 enhancement on cell apoptosis (**Fig. S1D**). Then, we examined apoptosis related protein expression, the results showed that FOXP1 inhibited Bax expression while promoting Bcl-2 expression, however, knockdown of XIST or overexpression of miR-506-3p had the opposite result (**Fig. S1E**). We also found that autophagy was promoted in the OE-FOXP1 group, while this change rescued in OE-FOXP1+miR-506-3p mimics and OE-FOXP1+sh-XIST groups (**Fig. S1F**). In addition, overexpression of FOXP1 increased LC3 II/I levels and decreased P62 levels, whereas miR-506-3p enhancement or XIST silencing restored these alterations (**Fig. S1G**). Overexpression of FOXP1 enhanced FOXP1, mTOR and p-AKT levels, while co-transfection of miR-506-3p mimics or sh-XIST eliminated the effect of OE-FOXP1

(**Fig. S1H**). These findings demonstrated that XIST/miR-506-3p/FOXP1 axis enhanced the carboplatin resistance of OC cells by regulating autophagy.

6. Knockdown of XIST impeded tumor growth through regulating FOXP1/AKT/mTOR pathway by targeting miR-506-3p in vivo

To verify the role of the novel axis, XIST/miR-506-3p/FOXP1 in vivo, we constructed mice models. We observed that XIST knockdown or carboplatin treatment repressed the volume and weight of the tumor, and the tumor growth was further inhibited in the sh-XIST+CBP group (**Fig. 5A-C**). Subsequently, we observed that knockdown of XIST or treatment of carboplatin suppressed the expression of XIST and FOXP1 in vivo, while up-regulating miR-506-3p expression (**Fig. 5D**). Moreover, the results from immunohistochemistry indicated that LC3 was down-regulated while caspase3 was up-regulated in mice models injected with XIST silenced SKOV3 cells or treated with carboplatin (**Fig. 5E**). Thus, silencing of XIST enhanced the sensitivity to carboplatin through the miR-506-3p/FOXP1 axis in vivo.
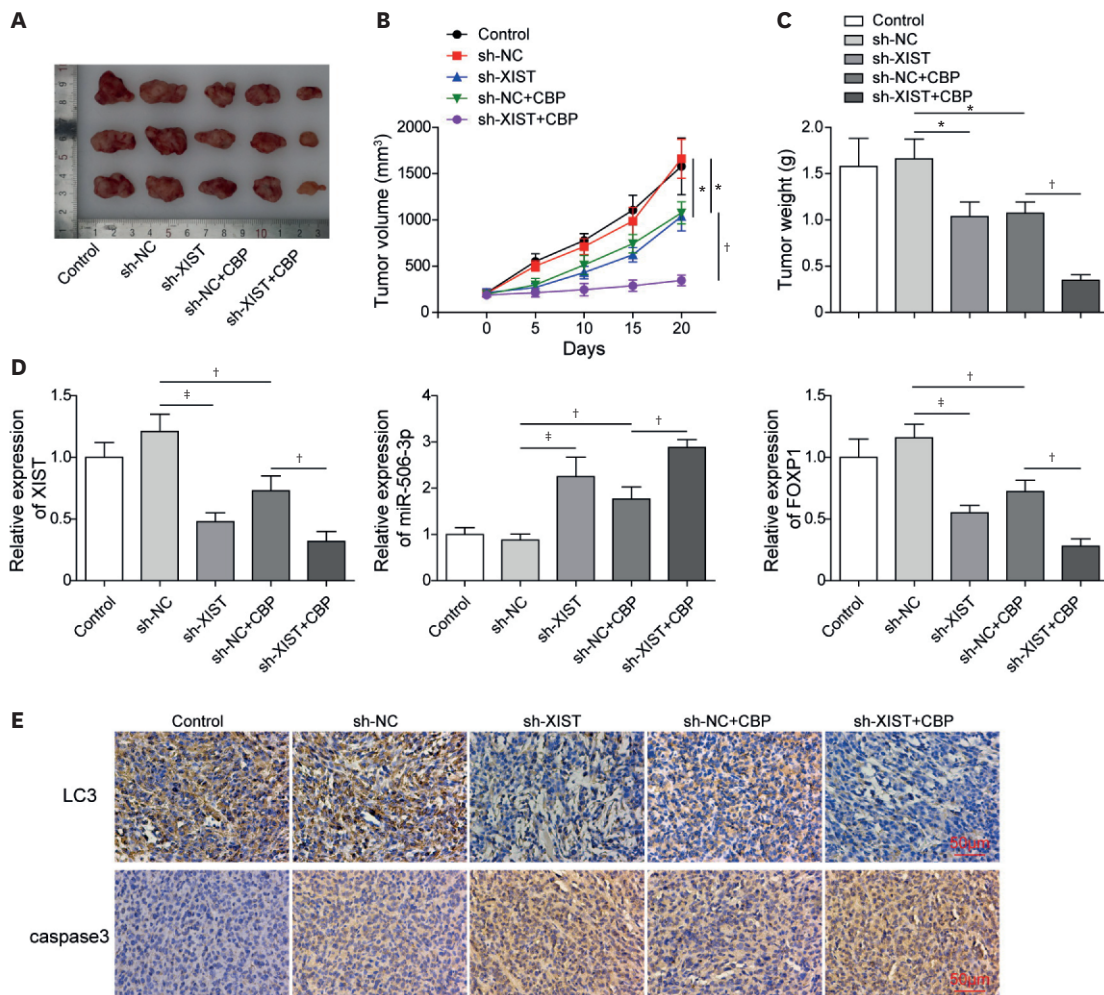

Fig. 5. Knockdown of XIST repressed tumor growth through regulating FOXP1/AKT/mTOR pathway by targeting miR-506-3p in vivo. (A-C) XIST silenced SKOV3 or SKOV3/CBP cells were injected to establish mice model and then the representative image, volume and weight of tumor were observed. (D) QRT-PCR evaluated XIST, miR-506-3p and FOXP1 expressions. (E) LC3 and caspase3 levels in subcutaneous xenograft mice model injected with SKOV3 or SKOV3/CBP cells transfected with sh-XIST was analyzed by immunohistochemistry. The data were showed as mean ± SD. n=6 per group.
AKT, protein kinase B; FOXP1, forkhead box protein P1; LC3, light chain 3; mTOR, mammalian target of rapamycin; sh-NC, short hairpin RNA NC; sh-XIST, short hairpin RNA XIST; XIST, X-inactive specific transcript.
*p<0.05, †p< 0.01, and ‡p<0.001.

DISCUSSION

Chemotherapy resistance has emerged as a significant stumbling block in the treatment of malignant tumor. The mechanism of drug resistance is complicated, which include tumor heterogeneity, reduced drug concentration to the target, alteration in drug target structure [18]. Carboplatin-based chemotherapy is the standard first-line treatment for OC patients, however, patients may relapse because of the developing carboplatin resistance [19]. Although the possible molecular mechanism of carboplatin resistance in OC had been elucidated by many publications [20,21], clinical experiments based on these studies have not yet yielded satisfactory therapeutic effects [22]. In this study, we found that knockdown of XIST suppressed the resistance of OC cells to carboplatin, investigated for the first time the roles of the XIST/miR-506/FOXP1 axis on carboplatin resistance in OC.

The dysregulation of lncRNAs was suggested to show vital effects in diverse processes of cancer development, including the initiation and progression [23]. In recent years, the publications of the functions of lncRNAs in drug resistance, such as the effect of lncRNA SNHG1 in sorafenib [24] and that of lncRNA PVT1 in gemcitabine [25], have also helped our understanding of tumor biology. The effect of XIST in drug resistance has also attracted increasing attention. For example, Schouten et al. suggested that XIST and 53BP1 could be used to identify patients with BRCA1-like breast cancer who have a high incidence and poor prognosis after high-dose chemotherapy [26]. Furthermore, XIST levels in OC were linked to the number of cancer stem cells (CSCs) and susceptibility to Taxol therapy [27]. We hypothesized that XIST affected carboplatin resistance in OC, and our results revealed that XIST promoted carboplatin resistance in vitro. Remarkably, XIST knockdown suppressed the autophagy. Autophagy was observed to be either tumor-suppressing or tumor-promoting in different cell context [28,29]. Autophagy induction has been shown to help cells survive stress, hypoxia and starvation. Furthermore, autophagy is also activated as a defensive mechanism to mediate the drug resistance of cancer therapy [30]. We concluded that XIST might affect OC cell resistance to carboplatin through regulating autophagy, which is in line with a prior study that inhibition of autophagy lowered the survival of CSCs during anticancer treatment [31]. In addition, carboplatin and XIST targeted therapy inhibited tumor growth in mice more effectively. These findings suggested that inhibition of XIST was a valuable therapeutic approach to enhance carboplatin sensitivity.

It is widely reported that lncRNA function as a ceRNA to bind specific miRNA, thereby regulating miRNA-mediated gene silencing [32]. To explore whether XIST could act as a ceRNA in OC carboplatin chemoresistance, we used bioinformatic analysis, RIP and dual-luciferase reporter assays, which observed XIST to engage in complementary binding with miR-506-3p. Thus, we hypothesized that XIST might modulate cell autophagy and OC cell resistance to carboplatin by serving as a miRNA sponge. More importantly, miR-506-3p was suggested to have important roles in cancer chemotherapy resistance regulation [14,33]. For example, overexpression of miR-506-5p reversed erlotinib resistance in non-small-cell lung cancer, which was mediated by suppressing the Sonic Hedgehog pathway [34]. Meanwhile, in our study, miR-506-3p silencing promoted carboplatin resistance cell growth and autophagy. The rescue experiments demonstrated that XIST silencing abolished the function of miR-506-3p knockdown in vitro, further indicating that XIST enhanced the resistance to carboplatin of OC cells by down-regulating miR-506-3p.

FOXP1 had been reported to positively regulate Bcl-2 levels, thereby affecting cell apoptosis [35] and acted as an oncogene in hepatocellular carcinoma [36], diffuse large B-cell lymphoma [37], and so on. In the study of OC, Li et al. [38] suggested that FOXP1 reversed the inhibition of miR-374b-5p on the proliferative, migration, and EMT abilities of OC cells, and the enhancement of miR-374b-5p on cell sensitivity to cisplatin. Furthermore, FOXP1 influenced autophagy and chemoresistance in OC through targeting miR-29c-3p [15]. Similarly, FOXP1 was targeted to miR-506-3p, and XIST knockdown or miR-506-3p enhancement abolished the promoting effects of FOXP1 overexpression on carboplatin resistance cell proliferation and autophagy in our work. In addition, we observed that FOXP1 overexpression upregulated AKT phosphorylation levels and mTOR expression, suggesting that FOXP1 contributed to the activation of the AKT/mTOR pathway, which was recognized as a key regulatory signal for autophagy [39]. Lee et al. [40] proved that carboplatin effectively suppressed the activation of the mTOR signaling cascade in OC cells. Therefore, we concluded that XIST knockdown inhibited autophagy and suppressed carboplatin resistance of OC cells through the FOXP1/AKT/mTOR pathway by targeting miR-506-3p. The biological functions of the XIST/miR-506-3p/FOXP1 pathway were also confirmed in vivo.

Finally, these findings firstly demonstrated that XIST/miR-506-3p/FOXP1 axis was involved in OC carboplatin resistance and regulated autophagy, providing a theoretical basis for XIST to be a prognostic marker for OC chemosensitivity.

ACKNOWLEDGEMENTS

SUPPLEMENTARY MATERIALS

Table S1
The primer sequences used in this study

Click here to view

Fig. S1
Knockdown of XIST inhibited autophagy and promoted the sensitivity of OC cells to carboplatin by regulating FOXP1/AKT/mTOR pathway via miR-506-3p. (A-B) QRT-PCR and western blot tested FOXP1 expression in SKOV3/CBP and A2780/CBP cells. OE-FOXP1, OE-FOXP1+miR-506-3p mimics or OE-FOXP1+sh-XIST was transfected into SKOV3/CBP and A2780/CBP cells, then (C-D) The cell viability and apoptosis were measured by colony formation, flow cytometry. (E) Western blot was performed to test the expression of Bax and Bcl-2. (F) Immunofluorescence assay measured the level of LC3. (G-H) The expression of LC3 II/I, P62, FOXP1, AKT, p-AKT and mTOR was detected. The data were showed as mean ± SD. n=3.

Click here to view

REFERENCES

1. Reid BM, Permuth JB, Sellers TA. Epidemiology of ovarian cancer: a review. Cancer Biol Med 2017;14:9-32.
   PUBMED | **CROSSREF**

2. Ferlay J, Soerjomataram I, Dikshit R, Eser S, Mathers C, Rebelo M, et al. Cancer incidence and mortality worldwide: sources, methods and major patterns in GLOBOCAN 2012. Int J Cancer 2015;136:E359-86.
   PUBMED | **CROSSREF**

3. Zeller C, Brown R. Therapeutic modulation of epigenetic drivers of drug resistance in ovarian cancer. Ther Adv Med Oncol 2010;2:319-29.
   PUBMED | **CROSSREF**

4. Herzog TJ. Recurrent ovarian cancer: how important is it to treat to disease progression? Clin Cancer Res 2004;10:7439-49.
   PUBMED | **CROSSREF**

5. Lin YH. Crosstalk of lncRNA and cellular metabolism and their regulatory mechanism in cancer. Int J Mol Sci 2020;21:E2947.
   PUBMED | **CROSSREF**

6. Zhu J, Kong F, Xing L, Jin Z, Li Z. Prognostic and clinicopathological value of long noncoding RNA XIST in cancer. Clin Chim Acta 2018;479:43-7.
   PUBMED | **CROSSREF**

7. Liu H, Deng H, Zhao Y, Li C, Liang Y. LncRNA XIST/miR-34a axis modulates the cell proliferation and tumor growth of thyroid cancer through MET-PI3K-AKT signaling. J Exp Clin Cancer Res 2018;37:279.
   PUBMED | **CROSSREF**

8. Zhao H, Wan J, Zhu Y. Carboplatin inhibits the progression of retinoblastoma through lncRNA XIST/miR-200a-3p/NRP1 axis. Drug Des Devel Ther 2020;14:3417-27.
   PUBMED | **CROSSREF**

9. Jiang R, Zhang H, Zhou J, Wang J, Xu Y, Zhang H, et al. Inhibition of long non-coding RNA XIST upregulates microRNA-149-3p to repress ovarian cancer cell progression. Cell Death Dis 2021;12:145.
   PUBMED | **CROSSREF**

10. Liz J, Esteller M. lncRNAs and microRNAs with a role in cancer development. Biochim Biophys Acta 2016;1859:169-76.
    PUBMED | **CROSSREF**

11. Kim JK, Kim TS, Basu J, Jo EK. MicroRNA in innate immunity and autophagy during mycobacterial infection. Cell Microbiol 2017;19:e12687.
    PUBMED | **CROSSREF**

12. Wang Y, Lei X, Gao C, Xue Y, Li X, Wang H, et al. MiR-506-3p suppresses the proliferation of ovarian cancer cells by negatively regulating the expression of MTMR6. J Biosci 2019;44:126.
    PUBMED | **CROSSREF**

13. Shi M, Zong X, Chen L, Guo X, Ding X. MiR-506-3p regulates autophagy and proliferation in post-burn skin fibroblasts through post-transcriptionally suppressing Beclin-1 expression. In Vitro Cell Dev Biol Anim 2020;56:522-32.
    PUBMED | **CROSSREF**

14. Sun Y, Wu J, Dong X, Zhang J, Meng C, Liu G. MicroRNA-506-3p increases the response to PARP inhibitors and cisplatin by targeting EZH2/β-catenin in serous ovarian cancers. Transl Oncol 2021;14:100987.
    PUBMED | **CROSSREF**

15. Hu Z, Cai M, Zhang Y, Tao L, Guo R. miR-29c-3p inhibits autophagy and cisplatin resistance in ovarian cancer by regulating FOXP1/ATG14 pathway. Cell Cycle 2020;19:193-206.
    PUBMED | **CROSSREF**

16. Ediriweera MK, Tennekoon KH, Samarakoon SR. Role of the PI3K/AKT/mTOR signaling pathway in ovarian cancer: Biological and therapeutic significance. Semin Cancer Biol 2019;59:147-60.
    PUBMED | **CROSSREF**

17. Bi E, Ma X, Lu Y, Yang M, Wang Q, Xue G, et al. Foxo1 and Foxp1 play opposing roles in regulating the differentiation and antitumor activity of T$_H$9 cells programmed by IL-7. Sci Signal 2017;10:eaak9741.
    PUBMED | **CROSSREF**

18. Damia G, Broggini M. Platinum resistance in ovarian cancer: role of DNA repair. Cancers (Basel) 2019;11:E119.
    PUBMED | **CROSSREF**

19. McGuire WP 3rd, Markman M. Primary ovarian cancer chemotherapy: current standards of care. Br J Cancer 2003;89 Suppl 3:S3-8.
    PUBMED | **CROSSREF**

20. Yoshida H, Teramae M, Yamauchi M, Fukuda T, Yasui T, Sumi T, et al. Association of copper transporter expression with platinum resistance in epithelial ovarian cancer. Anticancer Res 2013;33:1409-14.
    PUBMED

21. Ang JE, Gourley C, Powell CB, High H, Shapira-Frommer R, Castonguay V, et al. Efficacy of chemotherapy in BRCA1/2 mutation carrier ovarian cancer in the setting of PARP inhibitor resistance: a multi-institutional study. Clin Cancer Res 2013;19:5485-93.
    PUBMED | CROSSREF

22. Lee JM, Hays JL, Annunziata CM, Noonan AM, Minasian L, Zujewski JA, et al. Phase I/Ib study of olaparib and carboplatin in BRCA1 or BRCA2 mutation-associated breast or ovarian cancer with biomarker analyses. J Natl Cancer Inst 2014;106:dju089.
    PUBMED | CROSSREF

23. Munschauer M, Nguyen CT, Sirokman K, Hartigan CR, Hogstrom L, Engreitz JM, et al. Publisher Correction: The NORAD lncRNA assembles a topoisomerase complex critical for genome stability. Nature 2018;563:E32.
    PUBMED | CROSSREF

24. Li W, Dong X, He C, Tan G, Li Z, Zhai B, et al. LncRNA SNHG1 contributes to sorafenib resistance by activating the Akt pathway and is positively regulated by miR-21 in hepatocellular carcinoma cells. J Exp Clin Cancer Res 2019;38:183.
    PUBMED | CROSSREF

25. Zhou C, Yi C, Yi Y, Qin W, Yan Y, Dong X, et al. LncRNA PVT1 promotes gemcitabine resistance of pancreatic cancer via activating Wnt/β-catenin and autophagy pathway through modulating the miR-619-5p/Pygo2 and miR-619-5p/ATG14 axes. Mol Cancer 2020;19:118.
    PUBMED | CROSSREF

26. Schouten PC, Vollebergh MA, Opdam M, Jonkers M, Loden M, Wesseling J, et al. High XIST and low 53BP1 expression predict poor outcome after high-dose alkylating chemotherapy in patients with a BRCA1-like breast cancer. Mol Cancer Ther 2016;15:190-8.
    PUBMED | CROSSREF

27. Huang R, Zhu L, Zhang Y. XIST lost induces ovarian cancer stem cells to acquire taxol resistance via a KMT2C-dependent way. Cancer Cell Int 2020;20:436.
    PUBMED | CROSSREF

28. Li YY, Lam SK, Mak JC, Zheng CY, Ho JC. Erlotinib-induced autophagy in epidermal growth factor receptor mutated non-small cell lung cancer. Lung Cancer 2013;81:354-61.
    PUBMED | CROSSREF

29. Hippert MM, O'Toole PS, Thorburn A. Autophagy in cancer: good, bad, or both? Cancer Res 2006;66:9349-51.
    PUBMED | CROSSREF

30. Hu YL, Jahangiri A, Delay M, Aghi MK. Tumor cell autophagy as an adaptive response mediating resistance to treatments such as antiangiogenic therapy. Cancer Res 2012;72:4294-9.
    PUBMED | CROSSREF

31. Pagotto A, Pilotto G, Mazzoldi EL, Nicoletto MO, Frezzini S, Pastò A, et al. Autophagy inhibition reduces chemoresistance and tumorigenic potential of human ovarian cancer stem cells. Cell Death Dis 2017;8:e2943.
    PUBMED | CROSSREF

32. Thomson DW, Dinger ME. Endogenous microRNA sponges: evidence and controversy. Nat Rev Genet 2016;17:272-83.
    PUBMED | CROSSREF

33. Zhu J, Tao L, Jin L. MicroRNA-506-3p reverses gefitinib resistance in non-small cell lung cancer by targeting Yes-associated protein 1. Mol Med Rep 2019;19:1331-9.
    PUBMED

34. Haque I, Kawsar HI, Motes H, Sharma M, Banerjee S, Banerjee SK, et al. Downregulation of miR-506-3p facilitates EGFR-TKI resistance through induction of sonic hedgehog signaling in non-small-cell lung cancer cell lines. Int J Mol Sci 2020;21:E9307.
    PUBMED | CROSSREF

35. Sagaert X, de Paepe P, Libbrecht L, Vanhentenrijk V, Verhoef G, Thomas J, et al. Forkhead box protein P1 expression in mucosa-associated lymphoid tissue lymphomas predicts poor prognosis and transformation to diffuse large B-cell lymphoma. J Clin Oncol 2006;24:2490-7.
    PUBMED | CROSSREF

36. Zhang Y, Zhang S, Wang X, Liu J, Yang L, He S, et al. Prognostic significance of FOXP1 as an oncogene in hepatocellular carcinoma. J Clin Pathol 2012;65:528-33.
    PUBMED | CROSSREF

37. Lenz G, Wright GW, Emre NC, Kohlhammer H, Dave SS, Davis RE, et al. Molecular subtypes of diffuse large B-cell lymphoma arise by distinct genetic pathways. Proc Natl Acad Sci U S A 2008;105:13520-5.
PUBMED | CROSSREF

38. Li H, Liang J, Qin F, Zhai Y. MiR-374b-5p-FOXP1 feedback loop regulates cell migration, epithelial-mesenchymal transition and chemosensitivity in ovarian cancer. Biochem Biophys Res Commun 2018;505:554-60.
PUBMED | CROSSREF

39. Nicklin P, Bergman P, Zhang B, Triantafellow E, Wang H, Nyfeler B, et al. Bidirectional transport of amino acids regulates mTOR and autophagy. Cell 2009;136:521-34.
PUBMED | CROSSREF

40. Lee KB, Byun HJ, Park SH, Park CY, Lee SH, Rho SB. CYR61 controls p53 and NF-κB expression through PI3K/Akt/mTOR pathways in carboplatin-induced ovarian cancer cells. Cancer Lett 2012;315:86-95.
PUBMED | CROSSREF